Received: 9 May 2019 | Accepted: 23 December 2019

DOI: 10.1002/jcp.29434

Journal of Cellular Physiology WILEY

ORIGINAL RESEARCH ARTICLE

Phosphorylation of histone H4 at serine 1 is associated with GCN5 and mediates autophagy in osteosarcoma bone cell lines

Rui Jiang[1] | Ziyan Zhang[2] | Zhiwei Zhong[1] | Yuxuan Dai[1] | Guangyao Liu[1] | Chao Zhang[3]

[1]Department of Orthopaedics, China-Japan Union Hospital of Jilin University, Changchun, Jilin, China

[2]Department of Orthopaedics, The Second Hospital of Jilin University, Changchun, Jilin, China

[3]Department of Ophthalmology, The Second Hospital of Jilin University, Changchun, Jilin, China

Correspondence
Chao Zhang, Department of Ophthalmology, The Second Hospital of Jilin University, No. 218, Ziqiang Street, Changchun, 130041 Jilin, China.
Email: zhang0058zc@163.com

Abstract

Histone modification is critical for the process of autophagy in osteosarcoma. Whether phosphorylated histone H4 (H4) mediates autophagy remains to be seen. Here, we aimed to investigate the effects of general control nonderepressible 5 (GCN5)-evoked phosphorylation of H4 on autophagy. Osteosarcoma bone cell lines Saos-2, MG-63, and HOS cells were applied. Kinase activity was monitored in in vitro kinase assay buffer. Immunoprecipitation and glutathione S-transferase (GST) pull-down assay were exploited to confirm the association of GCN5 to H4. Furthermore, we determined green fluorescent protein (GFP)-tagged light chain 3 (LC3), long-lived protein, gene expression, and transcriptional activity. We found that a direct connection of GCN5 to H4 existed in osteosarcoma bone cells. Results indicated that GCN5 was implicated in the modulation of H4 phosphorylation at serine 1 (Ser1). GCN5-mediated phosphorylation of H4 at Ser1 facilitated the formation of GFP-LC3, conversion of LC3-I into LC3-II and transcriptional activity of autophagy-related genes. We reported that GCN5 was included in the modulation of H4 phosphorylation at Ser1. Fortification of epigenetic phosphorylated marks at Ser1 of H4 by GCN5 sensitized osteosarcoma bone cells to autophagy.

KEYWORDS
autophagy, GCN5, osteosarcoma, pSer1-H4

1 | INTRODUCTION

Autophagy is a homeostatic and conserved process in response to nutrient deprivation or metabolic stress (Russo & Russo, 2018). The complex role of autophagy in cancer continues to be elucidated since it both is a mechanism of tumor suppression and confers stress tolerance, which enables tumor cells to survive under adverse conditions (Singh et al., 2018). Many anticancer therapies have been found to trigger prosurvival autophagy, which presents a major impediment to successful chemotherapy (Fulda, 2018). In combination with autophagy inhibitors, the treatment resistance and tumor dormancy might be alleviated by genetic or pharmacological means to a great extent (Levy, Towers, & Thorburn, 2017; Wang, Hu, & Shen, 2016). As a consequence, understanding the role of autophagy in cancer treatment is critical, and it is also significant to address the mechanisms by which autophagy is induced.

General control nonderepressible 5 (GCN5) is identified as a transcription-related histone acetyltransferase, which associates histone acetylation with gene activation (Brownell et al., 1996). GCN5 exerts a paramount role as an acetyltransferase from hepatic gluconeogenesis (Dominy et al., 2012), telomere recombination (Jeitany et al., 2017), and nucleotide excision (Guo, Chen, Mitchell, & Johnson, 2011). In the onset and progression of cancers, GCN5 emerges as a mediator of oncogenic c-Myc and

proapoptotic E2F1 (Yin et al., 2015). GCN5-mediated acetylation facilitates proliferation-related gene expression in non-small-cell lung cancer (Zhao et al., 2018). Recent studies suggested that GCN5 may be a clinically relevant mechanism of cancer through histone modification (L. Chen et al., 2013). Of date, histone acetyltransferase inhibitor represses GCN5 expression and then impedes neuroblastoma cell growth, suggesting that GCN5 inhibitor has a potential in treating cancer (Gajer et al., 2015).

Histone modifications are implicated in the modulation of autophagy under metabolic stress in tumorigenesis (X. Li, Qian, & Lu, 2017; Stankov et al., 2014). For example, histone acetylation is induced to enhance the lysosome and autophagy-related gene (ATG) expression and preclude metabolic stress (X. Li et al., 2017). Histone posttranslational phosphorylation occurs to modulate DNA accessibility to transcription in response to genotoxic stress (Brehove et al., 2015; Millan-Zambrano et al., 2018). Recently, histone phosphorylation has been confirmed to directly regulate cellular adaption to stress in a transcription and chromatin manner (Bungard et al., 2010). The mammalian adenosine monophosphate–activated protein kinase activates the phosphorylation of histone H2B at serine 36 (Ser36), which next influences stress-dependent transcription (Bungard et al., 2010). In the vast majority of situations, GCN5 induces histone acetylation (Love, Sekaric, Shi, Grossman, & Androphy, 2012; Xue-Franzen, Henriksson, Burglin, & Wright, 2013). Newly, GCN5-induced cell-division Cycle 6 protein phosphorylation has been detected in the S phase of the cell cycle (Paolinelli, Mendoza-Maldonado, Cereseto, & Giacca, 2009). Nevertheless, whether GCN5 has a kinase activity remains to be seen.

In this study, we investigated whether GCN5 was implicated in the modulation of H4 phosphorylation. Besides, we aimed to verify whether GCN5/phosphorylated H4 at Ser1/ATGs epigenetic circuit was implicated in driving the autophagy process, which is necessary for the maintenance of the malignant state.

2 | MATERIALS AND METHODS

2.1 | Cells line and culture with stimuli

Human osteosarcoma bone cell lines HOS (Product No. CRL-1543™), MG-63 (Product No. CRL-1427™), and Sao-2 (Product No. HTB-85) were purchased from American Type Culture Collection (Rockville, MD) and cultured according to the supplier's recommendation. HOS were incubated in Dulbecco's modified Eagle' medium (DMEM) (Gibco, Gaithersburg, MD) supplemented with fetal bovine serum (FBS; Gibco) at a final concentration of 10% and 1% penicillin/streptomycin (Sigma-Aldrich, St. Louis, MO). MG-63 cells were maintained in DMEM supplemented with 10% FBS and 1% penicillin/streptomycin. Saos-2 cells were grown in McCoy's 5A medium (Gibco) containing 15% FBS and 1% penicillin/streptomycin. The cells were cultured in a humid atmosphere containing 5% CO_2 and 95% air at 37°C. Human embryonic kidney cell line HEK293 (RCB 1637; RIKEN BioResource Research Center, Koyadai, Tsukuba, Japan) cells were cultured in DMEM containing 10% FBS in an atmosphere containing 95% air and 5% CO_2 at 37°C. GCN5$^{-/-}$ and H4$^{-/-}$ MG-63 cells, H4$^{-/-}$ MG-63 cells, and GCN5$^{-/-}$ MG-63 cells were provided by Cyagen (Santa Clara, CA). To induce autophagy, MG-63 and HOS cells were cultured in Earle's balanced salt solutions (EBSS; Thermo Fisher Scientific, Waltham, MA) relative to complete medium for 2 hr. For blocking fusion of lysosomes with autophagosomes, the cells were treated with 20 μM chloroquine (Sigma-Aldrich) for 6 hr.

2.2 | Plasmids construct and transfection

GCN5 and H4 coding sequences were amplified by polymerase chain reaction (PCR) and the complementary DNA (cDNA) was ligated into pcDNATM3.1/V5-His-TOPO (Invitrogen, Carlsbad, CA) or pAd-Easy system (Invitrogen). Site-directed mutagenesis was performed to construct H4 mutants. H4 serine 1A was established to resist phosphorylation (H4 S1A). H4 serine 1D (H4 S1D) and H4 serine 1E (H4 S1E) were established to mimic phosphorylation. For downregulation of GCN5, siGCN5 (#1 and #2) was exploited to induce GCN5 silence. MG-63 was transfected with siATG. To induce ATGs silence, the cells were treated by 80 ng/ml doxycycline (Sigma-Aldrich) for 12 hr. Transfection was carried out with Lipofectamine 3000 (Invitrogen) according to the manufacturer's protocol.

2.3 | Immunoblotting assay

After transfection and incubation, the cells were harvested and lysed by lysis buffer in the presence of phosphatase inhibitor and protease inhibitors (Roche Applied Science, Indianapolis, IN). After size fractionation by sodium dodecyl sulfate-polyacrylamide gel electrophoresis (SDS-PAGE), the protein was transferred onto polyvinylidene difluoride membrane (Millipore, Bedford, MA) and blocked by 3% bovine serum albumin (BSA; Thermo Fisher Scientific). Next, the protein was incubated with the following primary antibodies, anti-HA tag antibody (an137838; 1:1,000; Abcam, Cambridge, UK), anti-phospho-H4 (Ser1) antibody (LS-C387542; 1:1,000; OriGene, Rockville, MD), anti-H4 antibody (223139; 1:1,000; USBiological, Salem, MA), anti-GCN5 antibody (222902; 1:1,000; USBiological), anti-GAPDH antibody (MBS9414022; 1:1,000; MyBioSource, San Diego, CA), anti-light chain 3 (LC3) antibody (orb500748; 1:1,000; Biorbyt, Cambridge, UK), anti-ATG-5 antibody (303136; 0.1 μg/ml; USBiological), anti-ATG-7 antibody (MBS619934; 1:1,000; MyBioSource), anti-ATG-13 antibody (220918; 1:1,000; USBiological) and anti-ATG-14 antibody (orb412630; 1:1,000; Biorbyt). The blots were then incubated with a horseradish peroxidase-conjugated secondary antibody (HAF008; 1:1,000; R&D Systems, Abingdon, UK). Finally, the signals were visualized by an enhanced chemiluminescence system according to the instructions (Thermo Fisher Scientific).

2.4 | Immunoprecipitation

After transfection, the cells were treated with 1% formaldehyde for 10 min at 37°C, and then 0.125 mol/L glycine solution was added. The cells were collected after washed with a 1 × phosphate-buffered saline (PBS) buffer (Sigma-Aldrich). The cell pellets were washed with washing buffer (0.25% Triton X-100, 10 mmol/L ethylenediaminetetraacetic acid [EDTA], 0.5 mmol/L egtazic acid [EGTA], and 10 mmol/L Tris [pH 8.0]), resuspended in sonication buffer (1 mmol/L EDTA, 0.5 mmol/L EGTA, and 10 mmol/L Tris [pH 8.0]), and subjected to sonication progress. The supernatant was collected and incubated with the indicated antibodies lined to agarose beads (Roche Applied Science) at 4°C for 16 hr. Immunoprecipitate was extensively washed and eluted with 2% SDS in $NaHCO_3$. Cross-link was reversed at 65°C for 4 hr and the eluate was treated with proteinase K (Roche Applied Science) at 45°C for 1 hr. The immunoprecipitate was then immunoblotted with antibodies against H4 and GCN5.

2.5 | Glutathione S-transferase pull-down assay

Glutathione S-transferase (GST) beads were loaded on the spin column and then equilibrated by PBS before usage (GE Healthcare, Madison, WI). The GST-GCN5 fusion protein was expressed in *Escherichia coli*. Then, the culture was lysed in lysis buffer by sonication. The resulting lysates were incubated with GST beads for 10 min at 4°C followed by centrifugation for 2 min (4,000*g*). Next, human histone H4 (14-697; Millipore) was incubated with the beads for 10 min on a rotating wheel at 4°C, and then the beads were washed with the washing buffer and centrifuged for 2 min (4,000*g*). The proteins were eluted by GST-elution buffer and finally immunoblotted with antibodies against H4.

2.6 | In vitro kinase assay

To assay the kinase activity, HA-tagged H4 were prepared from HEK293 cells. Briefly, HA-H4 (wild-type [WT] and S1A) plasmids were transfected into HEK293 cells and protein expression was induced by 0.1 mmol/L isopropyl β-d-1-thiogalactopyranoside at 37°C for 4 hr. HA-tagged protein was purified by Ni-NTA affinity column (QIAGEN, Hilden, Germany). Dialysis was performed overnight at 4°C with a dialysis kit (GE Healthcare). The homogeneity and concentration of these proteins were estimated by SDS-PAGE in combination with coomassie blue staining using BSA as a standard control. Next, GST-GCN5 (60–110 ng) prepared from *E. coli*. and HA-H4 (WT and S1A) (1.0–2.0 μg) were coincubated in kinase assay buffer containing 50 mM 4-(2-hydroxyethyl)-1-piperazineethanesulfonic acid (pH 7.5), 15 mM $MgCl_2$, 1 mM EGTA, 10% glycerol, 10 mM dithiothreitol, and 0.1 mM [γ-^{32}P]ATP (BLU002001MC; PerkinElmer, Waltham, MA) for 60 min at 30°C according to the manufacturer's protocol. EDTA was applied to stop the reaction. Then, the reaction was separated on SDS-PAGE. Finally, phosphoproteins were photographed using Phosphor-Image Screens (Fujifilm, Tokyo, Japan) and analyzed using the FLA-5000 Image Reader (Fujifilm). The separated proteins were immunoblotted with antibodies against phospho-H4 (Ser1), H4, and GCN5.

2.7 | Autophagy analysis

After transfection with mRFP-GFP-LC3 (Addgene, Watertown, MA) and incubation in EBSS with chloroquine, the cells were fixed with 4% paraformaldehyde and then observed under fluorescence microscopy (Olympus, Melville, NY). Approximately 100 transfected cells in 10–20 random fields were analyzed. The number of green fluorescent protein (GFP)-LC3 puncta per cell was counted. The number of autolysosomes was presented as the difference between GFP dots and RFP dots. The immunoblotting assay was performed with antibodies against the indicated proteins.

2.8 | Long-lived protein degradation analysis

To measure the rate of long-lived protein degradation, transfected HOS cells were labeled with l-[U-^{14}C]-valine at a concentration of 5 μCi/ml (PerkinElmer) in complete medium for 18 hr. Then, the cells were incubated with nonradioactive valine (10 mM; Sigma-Aldrich) for 18 hr. The medium was subsequently replaced with fresh medium with or without EBSS and cultured for 2 hr. Next, the culture was supplemented with 10% trichloroacetic acid (TCA; Thermo Fisher Scientific) and 1% PBS. After centrifugation (12,000 rpm, 10 min) at room temperature, trichloroacetic acid-soluble radioactivity was examined. Radioactivity in the pellet of cells was also detected. Protein breakdown was depicted as the ration of TCA-soluble radioactivity by total radioactivity.

2.9 | Gene expression analysis

To examine gene expression, total RNA was isolated from cells using TRIzol (Invitrogen) according to the manufacturer's protocol. cDNA was synthesized using 2 μg of RNA, random primers and High Capacity cDNA Reverse Transcription kit (Applied Biosystems, Foster City, CA). Quantitative real-time PCR was performed on the CFX384 Real-Time PCR system (Bio-Rad, Hercules, CA) and using Power SYBR Green PCR Master Mix (Applied Biosystems). Gene level was normalized to GAPDH and calculated using the $\Delta\Delta C_t$ method.

2.10 | Transcriptional activity assay

To evaluate the transcriptional activity of ATGs, we constructed the promoter region of ATG-5 and ATG-7 into the pGL3 luciferase reporter vector according to the manufacturer's instruction (Promega, Madison, WI). Simultaneous transfection was performed with GCN5 and H4 (WT and S1A). Luciferase

activity was measured using a Luminometer TD20/20 (Turner Designs, Sunnyvale, CA).

2.11 | Statistical analysis

All results were collected from three independent experiments with three replicates. Data were given as means ± standard derivation. Statistical analyses were performed with two-tailed Student's *t* test and one-way analysis of variance followed by Tukey's multiple comparisons test, and the null hypothesis was rejected at the 0.05 level. Statistical analyses were performed using the GraphPad Prism 6.0 statistical software (GraphPad, San Diego, CA).

3 | RESULTS

3.1 | Identification of H4 phosphorylation at Ser1 in human osteosarcoma cell lines

To investigate the phosphorylation state of H4 at Ser1 in human osteosarcoma bone cell lines, MG-63, HOS, and Saos-2 cells were subjected to immunoblotting assay. Compared with Saos-2 cells, robust H4 Ser1-phosphorylation was observed in osteosarcoma MG-63 and HOS cells, with a notable overexpression of GCN5 (Figure 1a), implying an association of GCN5 and H4 phosphorylation at Ser1. As it is unknown that GCN5 phosphorylates H4 at Ser1, we generated a GCN5-overexpressed or silenced MG-63 and HOS cells. Apparently, a higher proportion of phosphorylated H4 at Ser1 was detected by direct immunoblotting in GCN5-transfected cells than untransfected cells (Figure 1b). By contrast, no obvious phosphorylation of H4 at Ser1 was observed in GCN5-silenced cells (Figure 1c).

3.2 | GCN5 was involved in modulation of H4 phosphorylation at Ser1

To validate the direct combination of GCN5 with H4, GCN5 protein was immunoprecipitated with antibodies against GCN5, followed by proved with an antibody against H4. H4 was detected in GCN5 immunoprecipitate. Consistently, GCN5 was immunoblotted in H4 immunoprecipitate (Figure 2a). To determine the association of GCN5 with H4 at Ser1, point mutant construct of HA-tagged H4 lacking Ser1 site (S1A) was generated. GCN5 was combined with H4 WT protein but failed to bind to the H4 mutant protein (Figure 2b). To further elucidate the molecular mechanism, we performed a pull-down assay. GST-GCN5 was immobilized onto glutathione-sepharose resin, and bound proteins were analyzed by immunoblotting. GCN5-interacting protein H4 was presented in the pull-down assay (Figure 2c). To elucidate that H4 phosphorylation at Ser1 was associated with GCN5, in vitro kinase assay was performed, followed by immunoblotting assay. As shown in Figure 2d,e GCN5 was included in the modulation of H4 phosphorylation at Ser1.

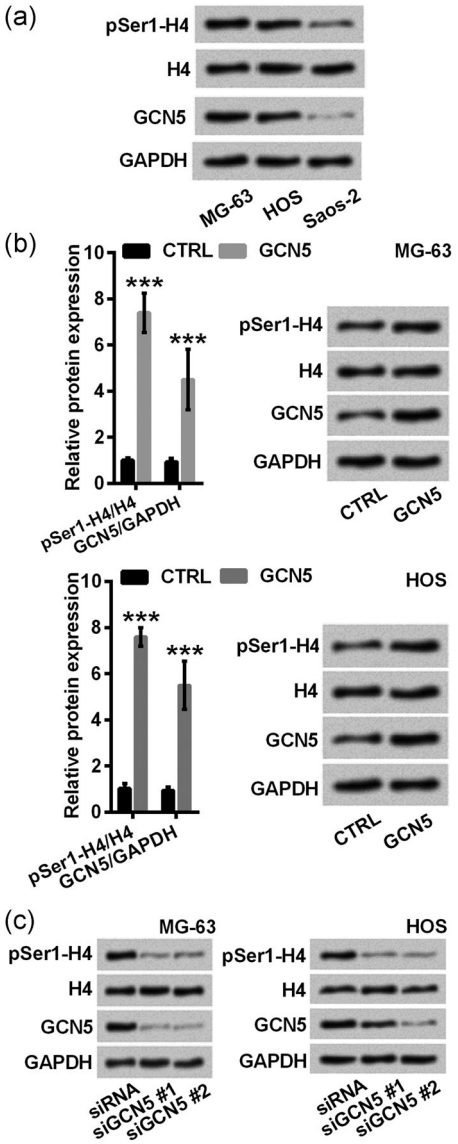

FIGURE 1 GCN5 overexpression drove the phosphorylation of H4 in human osteosarcoma cell lines. (a) Protein extract was subjected to immunoblotting with anti-phospho-H4 (Ser1), anti-H4, and ant-GCN5 antibodies. (b) GCN5 was transduced into MG-63 cells and HOS cells with empty plasmid-transfected cells as a control. Cell lysates were immunoblotted with the indicated antibodies. Relative protein expression was normalized to GAPDH. $p < .001$. (c) Small interfering RNAs (siRNAs) (#1 and #2) were transduced into MG-63 and HOS cells for silencing GCN5. Proteins were collected for immunoblotting with the indicated antibodies. $n = 3$. Ctrl, control; GCN5, general control nonderepressible 5; Ser1, serine 1

3.3 | GCN5 was required to induce autophagy in starved environment

To verify a direct role of GCN5 in autophagy, GCN5 was overexpressed in MG-63 and HOS cells. To initiate starvation-based autophagy, the cells were treated with EBSS. As indicated

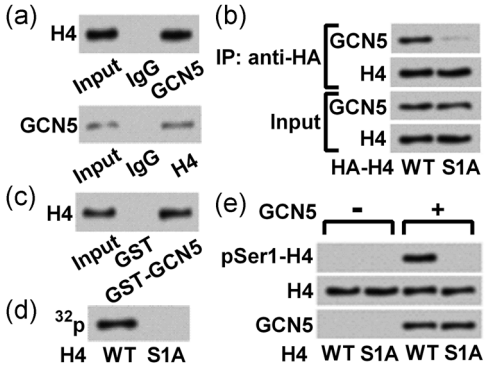

FIGURE 2 H4 phosphorylation at Ser1 required GCN5. (a) Immunoblotting analysis was performed to examine the interaction between H4 phosphorylation and GCN5. GCN5 or H4 was immunoprecipitated with GCN5 antibody or H4-antibody-conjugated beads, respectively. (b) HOS cells were infected with HA-H4 (WT and S1A). HA-H4 was immunoprecipitated with HA-antibody conjugated beads. Immunoblotting was performed using antibodies against GCN5 and H4. (c) GST-GCN5 was prepared in *Escherichia coli*. GST pull-down assay was carried out for testing the association between GCN5 and H4. (d) In vitro kinase assay was carried out by incubating GCN5 protein from *E. coli*. with H4 (WT and S1A) from HEK293 cells in the presence of ^{32}P. (e) Immunoblotting analysis of H4 phosphorylation status in in vitro kinase assay system was carried out. $n = 3–5$. GCN5, general control nonderepressible 5; IgG, immunoglobulin G; Ser1, serine 1; WT, wild-type

in Figure 3a, EBSS resulted in an evident increase in the number of autophagosomes ($p < .01$), whereas in untransfected cells, the number of autophagosomes was decreased ($p < .01$). Results from immunoblotting assay (Figure 3b) suggested that EBSS treatment resulted in the abundance of GCN5 as well as the degradation of LC3-II into LC3-I in GCN5-overexpressed cells. In contrast, EBSS has a modest effect on LC3-II expression in untransfected cells (Figure 3b). Next, to confirm that GCN5 was implicated in autophagy through a blockage of autophagosomes formation manner, the cells were administrated with late-stage autophagy inhibitor (chloroquine). As shown in Figure 3c, GFP-LC3 protein was visibly accumulated after EBSS induction in WT cells ($p < .01$) while not significantly expressed in untransfected cells ($p < .01$). We further assessed the autophagy by assaying the degradation of long-lived proteins. Evidently, EBSS accelerated ($p < .01$) the rate of autophagy-modulated degradation in GCN5-overexpressed cells. EBSS-induced degradation was not apparently ($p < .01$) in untransfected cells (Figure 3d). The expression of proteins implicated in autophagy was further determined. As indicated in Figure 3e, GCN5 overexpression resulted in the abundance of ATGs (ATG-5, ATG-13, and ATG-14) as well as LC3-II, while LC3-II expression was attenuated by doxycycline-induced silence of ATGs.

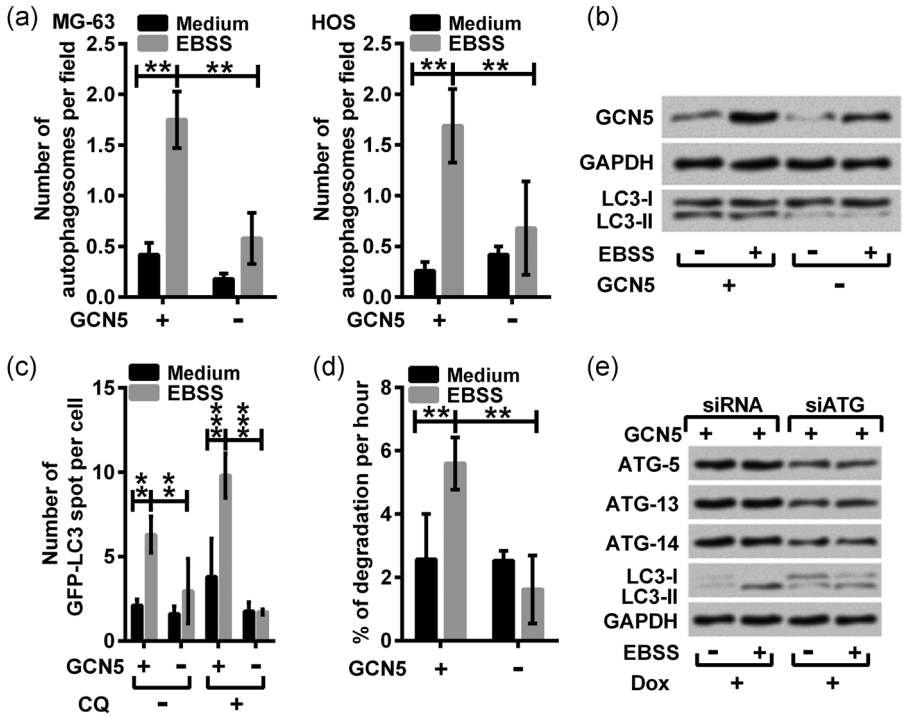

FIGURE 3 GCN5-mediated autophagy in osteosarcoma cells. (a) GCN5 was transfected into MG-63 and HOS cells. The cells were cultured in EBSS for the induction of autophagy. $^{**}p < .01$. (b) MG-63 cells were infected with GCN5 and incubated in EBSS. The cell lysate was collected for immunoblotting assay with antibodies against GCN5, LC3-I, and LC3-II. (c) MG-63 cells were cotransfected GCN5 and GFP-LC3. The cells were maintained in EBSS with or without chloroquine (CQ). GFP-LC3 puncta were observed or counted with fluorescence microscopy. $^{**}p < .01$, $^{***}p < .01$. (d) Long-lived protein was radioactively labeled in GCN5-transfected MG-63 cells. After incubation in EBSS, protein degradation was determined and depicted as the rate of degradation of long-lived proteins. $^{**}p < .01$. (e) MG-63 cells were cotransfected with siATG and GCN5 and cultured in EBSS. Doxycycline (Dox) was used to induce ATG silence. Immunoblotting was carried out with antibodies against the indicated proteins. $n = 3–5$. ATG, autophagy-related genes; EBSS, Earle's balanced salt solutions; GCN5, general control nonderepressible 5; GFP, green fluorescent protein; LC, light chain; siRNA, small interfering RNA

3.4 | GCN5 kinase activity-mediated H4 Ser1-phosphorylation was implicated in starvation-induced autophagy

To confirm that GCN5-mediated Ser1-phosphorylation of H4 modulates autophagy, $H4^{-/-}$ MG-63 cells were established and transfected with H4 (WT and S1A). Ser1-phosphorylated H4 expression was obviously dampened in H4 S1A (Figure 4a). EBSS obviously ($p < .05$) induced the accumulation of GFP-LC3, which was more significant ($p < .01$) in H4 WT-transfected cells. By contrast, the number of GFP-LC3 was remarkably ($p < .05$) reduced by H4 S1A, which was resistant to phosphorylation (Figure 4b). To further examine the consequences of GCN5-evoked phosphorylation, immunoblotting analysis was performed in $GCN5^{-/-}$ MG-63 cells. As shown in Figure 4c, a distinct increase in the expression of LC3-II was observed in GCN5-transfected cells following EBSS treatment. Next, we enforced GCN5 overexpression in MEG-63 cells followed by starvation induction, and an increase in Ser1-phosphorylated H4 was seen in H4 WT-transfected cells while it was decreased in H4 S1A-transfected cells (Figure 4d). Furthermore, GCN5-mediated phosphorylation of H4 could lead to the accumulation of GFP-LC3 ($p < .05$; Figure 4e).

3.5 | GCN5-mediated phosphorylation of H4 at Ser1 was involved in transcriptional modulation of ATGs

To investigate the relevance of H4 phosphorylation on ATG messenger RNA (mRNA) and protein expression, we constructed Ser1-phosphorylated H4-overexpressed MG-63 cells (H4 S1D and S1E). Clearly, EBSS facilitated the mRNA expression of ATG-5 ($p < .01$) and ATG-7 ($p < .01$), while it was not significantly increased in GCN5-deficient cells ($p > .05$). However, H4 S1D and S1E contributed to the increase in the mRNA level of ATG-5 ($p < .05$) and ATG-7 ($p < .05$) (Figure 5a). Consistently, the protein level of ATG-5 and ATG-7 was enhanced by Ser1-phosphorylated H4 (Figure 5b). In addition, luciferase assay suggested that EBSS-induced transcriptional activity ($p < .05$) of ATG-5 and ATG-7 was further fortified by GCN5-mediated phosphorylation of H4 ($p < .01$) (Figure 5c). Moreover, protein levels of ATG-5 and ATG-7 were visibly enhanced in Ser1-phosphorylated H4-overexpressed cells (Figure 5d). Meanwhile, the conversion of LC3-I to LC3-II was promoted by GCN5-mediated phosphorylation of H4 (Figure 5d). As a consequence, GCN5-evoked phosphorylation of H4 facilitated the transcriptional activity of ATGs implicated in autophagy.

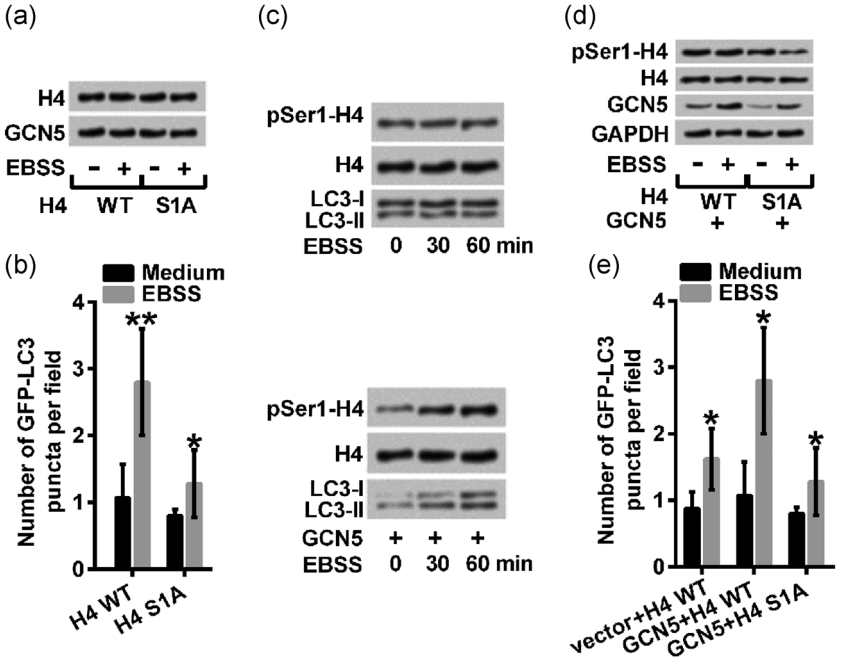

FIGURE 4 GCN5 modulated autophagy via phosphorylating H4 at Ser1. $H4^{-/-}$ MG-63 cells were transfected with H4 (WT and S1A). (a) Immunoblotting was performed with the indicated antibodies after autophagy induction using EBSS. (b) GFP-LC3 was introduced into the cells and GFP-LC3 puncta were observed using fluorescence microscopy after autophagy induction. $^{*}p < .05$, $^{**}p < .01$. (c) $GCN5^{-/-}$ MG-63 cells were transfected with or without GCN5 and incubated in EBSS. Cell lyse was immunoblotting with antibodies against the indicated proteins. $H4^{-/-}$ and $GCN5^{-/-}$ MG-63 cells were transfected with the indicated plasmids. (d) The immunoblotting assay was performed with antibodies against the indicated proteins under a starved condition. (e) GFP-LC3 puncta were observed and counted with fluorescence microscopy after autophagy induction. $^{*}p < .05$. $n = 3–5$. EBSS, Earle's balanced salt solutions; GCN5, general control nonderepressible 5; GFP, green fluorescent protein; LC, light chain; WT, wild-type

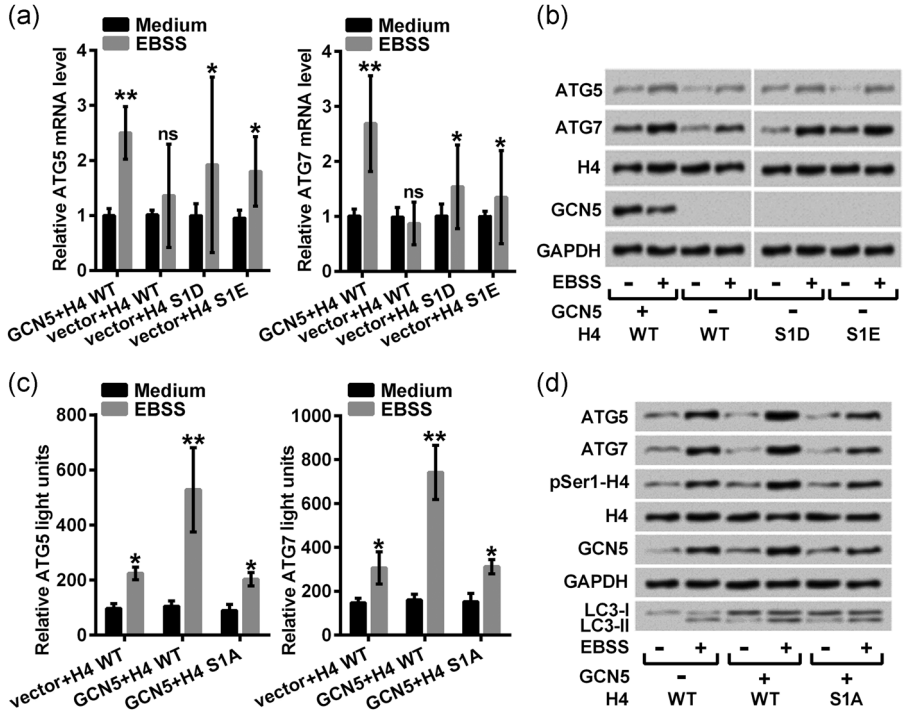

FIGURE 5 GCN5-mediated phosphorylation of H4 at serine 1 promoted autophagy by regulating ATGs expression. $H4^{-/-}$ and $GCN5^{-/-}$ MG-63 cells were transfected with the indicated plasmids and cultured in EBSS. (a) ATG-5 and ATG-7 mRNA expression were evaluated by qRT-PCR. $^{ns}p > .05$, $^{*}p < .05$, $^{**}p < .01$. (b) The immunoblotting assay was performed with antibodies against the indicated proteins. $H4^{-/-}$ and $GCN5^{-/-}$ MG-63 cells were transfected with the indicated plasmids. (c) Luciferase activity was examined using a turner design luminometer which presented gene transcriptional activity. $^{*}p < .05$, $^{**}p < .01$. (d) The immunoblotting assay was performed with antibodies against the indicated proteins. $n = 3–5$. ATG, autophagy-related genes; EBSS, Earle's balanced salt solutions; GCN5, general control nonderepressible 5; mRNA, messenger RNA; qRT-PCR, quantitative real-time polymerase chain reaction; WT, wild-type

4 | DISCUSSION

Here, we uncovered that GCN5 participated in modulation phosphorylation of H4 at Ser1. Furthermore, we have demonstrated that phosphorylated H4 at Ser1 by GCN5 sustained the expression of ATGs and LC3-II formation which were essential for autophagy. Collectively, these results illustrated activating of autophagy pathways by GCN5 underlay its effectiveness in driving the autophagy of osteosarcoma cells.

Osteosarcoma is recognized as an aggressive cancer mainly occurring in children and adolescents. Its treatment relies on surgery and chemotherapy (Isakoff, Bielack, Meltzer, & Gorlick, 2015). In the contest of osteosarcoma, autophagy is required to meet the high energy demand of unrestrained proliferation in various stress or resist starved, hypoxic, and chemotherapeutic stresses in tumor cells (Camuzard, Santucci-Darmanin, Carle, & Pierrefite-Carle, 2019). GCN5 has recently been reported to play a promoting role in the progression of malignant tumors (Majaz et al., 2016), primarily dependent on GCN5-mediated acetylation (L. Li, Liu, Zhang, & Ye, 2015; Zhao et al., 2018). Mostly, GCN5 functions as a histone acetyltransferase in the modulation of gene expression (J. Chen et al., 2010). Interesting, a recent study has shown that GCN5 indirectly mediates site-specific phosphorylation of cell-division Cycle 6 during the relocalization of protein to the cell cytoplasm (Paolinelli et al., 2009). Our results first demonstrated an association of GCN5 with the phosphorylation of H4 at Ser1.

As predicted using the Conserved Domains tool (https://www.ncbi.nlm.nih.gov/Structure/cdd/wrpsb.cgi), GCN5 protein (GeneBank: AAC39769.1) is annotated with P300/CBP-associated factor N-terminal domain, Bromodomain, and transcription factor involved in chromatin remodeling, which is classified as a model that spans more than one domain and contains Bromodomain. Currently, Bromodomain (726-834) has been widely confirmed in GCN5 in acetylated H4 (Ornaghi, Ballario, Lena, Gonzalez, & Filetici, 1999; Owen et al., 2000) while there are few reports on other domains. A previous study found Ser10 phosphorylation in H3 is associated with lysine 14 acetylation by GCN5, implying that multiple covalent modifications functionally mediate transcriptional regulation (Lo et al., 2000). Considering that both acetylation and phosphorylation of H4 are implicated in the autophagy process, we tried to figure out whether this relationship exerted a role in autophagy (Fullgrabe et al., 2013; Liu et al., 2019). Besides, a previous study showed that histone acetyltransferase GCN5 is in conjunction with histone kinase Snf1 to control gene transcription (Lo et al., 2001). Here, we straight focused on whether GCN5 regulated H4 phosphorylation and whether GCN5 regulated autophagy through this phosphorylation.

Autophagy involves the formation of autophagosomes and fusion with lysosomes (Bento et al., 2016). Chloroquine is an autophagy inhibitor by blocking the fusion of autophagosomes with lysosomes, which has been clinically applied with chemotherapy (Golden et al., 2014). We found the blocking effects were notably retarded in GCN5-deficient cells. More than that, GCN5 favored ATGs expression and LC3-II formation. The initiation of autophagy is controlled by the ATG-1 kinase complex, consisting of ATG-1, ATG-13, and ATG-17 (Wesselborg & Stork, 2015). During the initiation phase of autophagy, ATG-5-ATG-12-ATG-16 complex converses LC3-I into LC3-II by an ATG-7 and ATG-3-dependent cascade. LC3-II is commonly applied to monitor autophagy. ATG-14 promotes the fusion of autophagosome to endolysosome (Diao et al., 2015). Our results showed that EBSS drove the formation of GCN5 that was ultimately conducive to promote autophagosome formation with an accumulation of LC3-II. An unexpected finding that has emerged from our study was the ATGs silence-caused downregulation of LC3-II in GCN5-overexpressed cells, suggesting that GCN5 might mediate autophagy by modulation of ATGs. Of note, GCN5 acetylates autophagy protein ATG-7 in response to light- and nitrogen-starvation-induced autophagy in *Magnaporthe oryzae* (Zhang et al., 2017). This is consistent with our reports demonstrating a role for GCN5 in the modulation of autophagy in osteosarcoma cells.

Generally, it has been uncovered that H4 mediates the outcome of autophagy in an acetylated form (Ahn & Yoon, 2017; Fullgrabe et al., 2013). As for the biological function of its phosphorylated form, the phosphorylation of H4 at Ser47 modulates nucleosome assembly (Kang et al., 2011). It has been reported that tyrosine 88-phosphorylated H4 drives castration-resistant in prostate cancer for the maintenance of the malignant state (Mahajan et al., 2017). Casein kinase 2α-mediated phosphorylation of H4 at Ser1 antagonizes H4 N-α-terminal acetylation, which might inhibit the epithelial-to-mesenchymal transition of lung cancer (Ju et al., 2017). Here we found GCN5-mediated phosphorylation of H4 at Ser1 underlies its effectiveness in invoking autophagy. Our assessment of autophagy-associated protein expression revealed GCN5-mediated phosphorylation was involved in the modulation of autophagosome formation. Besides these important modulatory effects on cellular activities, phosphorylated H4 at Ser1 marks the genome, which participates in chromosome condensation in eukaryotes (Krishnamoorthy et al., 2006). The functions and mechanisms of phosphorylated H4 Ser1 are required to be further elucidated.

5 | CONCLUSION

Our data not only provided evidence that H4 phosphorylation at Ser1 required GCN5 for the autophagy process but also suggested that this phosphorylation promoted ATGs expression and LC3-II formation. Furthermore, it would be an underlying mechanism thereby osteosarcoma cells were sensitive to EBSS-induced autophagy. Overall, uncovering GCN5-mediated phosphorylation of H4 has substantial potential to advance a therapeutic option for osteosarcoma.

CONFLICT OF INTERESTS

The authors declare that there are no conflict of interests.

AUTHOR CONTRIBUTIONS

R. J. conceived and designed the experiments; Z. Y. Z. and Z. W. Z. performed the experiments and analyzed the data; Y. X. D. and G. Y. L. contributed reagents/materials/analysis tools; and C. Z. wrote and revised the manuscript.

DATA AVAILABILITY STATEMENT

The dataset(s) supporting the conclusions of this article is(are) included within the article.

ORCID

Chao Zhang http://orcid.org/0000-0002-2240-2639

REFERENCES

Ahn, M. Y., & Yoon, J. H. (2017). Histone deacetylase 7 silencing induces apoptosis and autophagy in salivary mucoepidermoid carcinoma cells. *Journal of Oral Pathology & Medicine*, *46*(4), 276–283.

Bento, C. F., Renna, M., Ghislat, G., Puri, C., Ashkenazi, A., Vicinanza, M., … Rubinsztein, D. C. (2016). Mammalian autophagy: How does it work? *Annual Review of Biochemistry*, *85*, 685–713.

Brehove, M., Wang, T., North, J., Luo, Y., Dreher, S. J., Shimko, J. C., … Poirier, M. G. (2015). Histone core phosphorylation regulates DNA accessibility. *The Journal of Biological Chemistry*, *290*(37), 22612–22621.

Brownell, J. E., Zhou, J., Ranalli, T., Kobayashi, R., Edmondson, D. G., Roth, S. Y., & Allis, C. D. (1996). Tetrahymena histone acetyltransferase A: A homolog to yeast Gcn5p linking histone acetylation to gene activation. *Cell*, *84*(6), 843–851.

Bungard, D., Fuerth, B. J., Zeng, P. Y., Faubert, B., Maas, N. L., Viollet, B., … Berger, S. L. (2010). Signaling kinase AMPK activates stress-promoted transcription via histone H2B phosphorylation. *Science*, *329*(5996), 1201–1205.

Camuzard, O., Santucci-Darmanin, S., Carle, G. F., & Pierrefite-Carle, V. (2019). Role of autophagy in osteosarcoma. *Journal of Bone Oncology*, *16*, 100235.

Chen, J., Luo, Q., Yuan, Y., Huang, X., Cai, W., Li, C., … Li, B. (2010). Pygo2 associates with MLL2 histone methyltransferase and GCN5 histone acetyltransferase complexes to augment Wnt target gene expression and breast cancer stem-like cell expansion. *Molecular and Cellular Biology*, *30*(24), 5621–5635.

Chen, L., Wei, T., Si, X., Wang, Q., Li, Y., Leng, Y., … Kang, J. (2013). Lysine acetyltransferase GCN5 potentiates the growth of non-small cell lung cancer via promotion of E2F1, cyclin D1, and cyclin E1 expression. *The Journal of Biological Chemistry*, *288*(20), 14510–14521.

Diao, J., Liu, R., Rong, Y., Zhao, M., Zhang, J., Lai, Y., … Zhong, Q. (2015). ATG14 promotes membrane tethering and fusion of autophagosomes to endolysosomes. *Nature*, *520*(7548), 563–566.

Dominy, J. E., Jr., Lee, Y., Jedrychowski, M. P., Chim, H., Jurczak, M. J., Camporez, J. P., … Puigserver, P. (2012). The deacetylase Sirt6 activates the acetyltransferase GCN5 and suppresses hepatic gluconeogenesis. *Molecular Cell*, *48*(6), 900–913.

Fulda, S. (2018). Targeting autophagy for the treatment of cancer. *Biological Chemistry*, *399*(7), 673–677.

Fullgrabe, J., Lynch-Day, M. A., Heldring, N., Li, W., Struijk, R. B., Ma, Q., … Joseph, B. (2013). The histone H4 lysine 16 acetyltransferase hMOF regulates the outcome of autophagy. *Nature*, *500*(7463), 468–471.

Gajer, J. M., Furdas, S. D., Grunder, A., Gothwal, M., Heinicke, U., Keller, K., … Jung, M. (2015). Histone acetyltransferase inhibitors block neuroblastoma cell growth in vivo. *Oncogenesis*, *4*, e137.

Golden, E. B., Cho, H. Y., Jahanian, A., Hofman, F. M., Louie, S. G., Schonthal, A. H., & Chen, T. C. (2014). Chloroquine enhances temozolomide cytotoxicity in malignant gliomas by blocking autophagy. *Neurosurgical Focus*, *37*(6), E12.

Guo, R., Chen, J., Mitchell, D. L., & Johnson, D. G. (2011). GCN5 and E2F1 stimulate nucleotide excision repair by promoting H3K9 acetylation at sites of damage. *Nucleic Acids Research*, *39*(4), 1390–1397.

Isakoff, M. S., Bielack, S. S., Meltzer, P., & Gorlick, R. (2015). Osteosarcoma: Current treatment and a collaborative pathway to success. *Journal of Clinical Oncology*, *33*(27), 3029–3035.

Jeitany, M., Bakhos-Douaihy, D., Silvestre, D. C., Pineda, J. R., Ugolin, N., Moussa, A., … Boussin, F. D. (2017). Opposite effects of GCN5 and PCAF knockdowns on the alternative mechanism of telomere maintenance. *Oncotarget*, *8*(16), 26269–26280.

Ju, J., Chen, A., Deng, Y., Liu, M., Wang, Y., Wang, Y., … Zhao, Q. (2017). NatD promotes lung cancer progression by preventing histone H4 serine phosphorylation to activate Slug expression. *Nature Communications*, *8*(1), 928.

Kang, B., Pu, M., Hu, G., Wen, W., Dong, Z., Zhao, K., … Zhang, Z. (2011). Phosphorylation of H4 Ser 47 promotes HIRA-mediated nucleosome assembly. *Genes & Development*, *25*(13), 1359–1364.

Krishnamoorthy, T., Chen, X., Govin, J., Cheung, W. L., Dorsey, J., Schindler, K., … Berger, S. L. (2006). Phosphorylation of histone H4 Ser1 regulates sporulation in yeast and is conserved in fly and mouse spermatogenesis. *Genes & Development*, *20*(18), 2580–2592.

Levy, J. M. M., Towers, C. G., & Thorburn, A. (2017). Targeting autophagy in cancer. *Nature Reviews Cancer*, *17*(9), 528–542.

Li, L., Liu, B., Zhang, X., & Ye, L. (2015). The oncoprotein HBXIP promotes migration of breast cancer cells via GCN5-mediated microtubule acetylation. *Biochemical and Biophysical Research Communications*, *458*(3), 720–725.

Li, X., Qian, X., & Lu, Z. (2017). Local histone acetylation by ACSS2 promotes gene transcription for lysosomal biogenesis and autophagy. *Autophagy*, *13*(10), 1790–1791.

Liu, Y., Long, Y. H., Wang, S. Q., Zhang, Y. Y., Li, Y. F., Mi, J. S., … Zhang, X. J. (2019). JMJD6 regulates histone H2A.X phosphorylation and promotes autophagy in triple-negative breast cancer cells via a novel tyrosine kinase activity. *Oncogene*, *38*(7), 980–997.

Lo, W. S., Duggan, L., Emre, N. C., Belotserkovskya, R., Lane, W. S., Shiekhattar, R., & Berger, S. L. (2001). Snf1--a histone kinase that works in concert with the histone acetyltransferase Gcn5 to regulate transcription. *Science*, *293*(5532), 1142–1146.

Lo, W. S., Trievel, R. C., Rojas, J. R., Duggan, L., Hsu, J. Y., Allis, C. D., … Berger, S. L. (2000). Phosphorylation of serine 10 in histone H3 is functionally linked in vitro and in vivo to Gcn5-mediated acetylation at lysine 14. *Molecular Cell*, *5*(6), 917–926.

Love, I. M., Sekaric, P., Shi, D., Grossman, S. R., & Androphy, E. J. (2012). The histone acetyltransferase PCAF regulates p21 transcription through stress-induced acetylation of histone H3. *Cell Cycle*, *11*(13), 2458–2466.

Mahajan, K., Malla, P., Lawrence, H. R., Chen, Z., Kumar-Sinha, C., Malik, R., … Mahajan, N. P. (2017). ACK1/TNK2 regulates histone H4 Tyr88-phosphorylation and AR gene expression in castration-resistant prostate cancer. *Cancer Cell*, *31*(6), 790–803.e798.

Majaz, S., Tong, Z., Peng, K., Wang, W., Ren, W., Li, M., … Yu, C. (2016). Histone acetyl transferase GCN5 promotes human hepatocellular carcinoma progression by enhancing AIB1 expression. *Cell & Bioscience*, *6*, 47.

Millan-Zambrano, G., Santos-Rosa, H., Puddu, F., Robson, S. C., Jackson, S. P., & Kouzarides, T. (2018). Phosphorylation of histone H4T80 triggers DNA damage checkpoint recovery. *Molecular Cell*, *72*(4), 625.e4–635.e4.

Ornaghi, P., Ballario, P., Lena, A. M., Gonzalez, A., & Filetici, P. (1999). The bromodomain of Gcn5p interacts in vitro with specific residues in the N terminus of histone H4. *Journal of Molecular Biology*, *287*(1), 1–7.

Owen, D. J., Ornaghi, P., Yang, J. C., Lowe, N., Evans, P. R., Ballario, P., … Travers, A. A. (2000). The structural basis for the recognition of acetylated histone H4 by the bromodomain of histone acetyltransferase gcn5p. *The EMBO Journal*, *19*(22), 6141–6149.

Paolinelli, R., Mendoza-Maldonado, R., Cereseto, A., & Giacca, M. (2009). Acetylation by GCN5 regulates CDC6 phosphorylation in the S phase of the cell cycle. *Nature Structural & Molecular Biology*, *16*(4), 412–420.

Russo, M., & Russo, G. L. (2018). Autophagy inducers in cancer. *Biochemical Pharmacology*, *153*, 51–61.

Singh, S. S., Vats, S., Chia, A. Y., Tan, T. Z., Deng, S., Ong, M. S., … Kumar, A. P. (2018). Dual role of autophagy in hallmarks of cancer. *Oncogene*, *37*(9), 1142–1158.

Stankov, M. V., El Khatib, M., Kumar Thakur, B., Heitmann, K., Panayotova-Dimitrova, D., Schoening, J., … Klusmann, J. H. (2014). Histone deacetylase inhibitors induce apoptosis in myeloid leukemia by suppressing autophagy. *Leukemia*, *28*(3), 577–588.

Wang, C., Hu, Q., & Shen, H. M. (2016). Pharmacological inhibitors of autophagy as novel cancer therapeutic agents. *Pharmacological Research*, *105*, 164–175.

Wesselborg, S., & Stork, B. (2015). Autophagy signal transduction by ATG proteins: From hierarchies to networks. *Cellular and Molecular Life Sciences*, *72*(24), 4721–4757.

Xue-Franzen, Y., Henriksson, J., Burglin, T. R., & Wright, A. P. (2013). Distinct roles of the Gcn5 histone acetyltransferase revealed during transient stress-induced reprogramming of the genome. *BMC Genomics*, *14*, 479.

Yin, Y. W., Jin, H. J., Zhao, W., Gao, B., Fang, J., Wei, J., … Fang, D. (2015). The histone acetyltransferase GCN5 expression is elevated and regulated by c-Myc and E2F1 transcription factors in human colon cancer. *Gene Expression*, *16*(4), 187–196.

Zhang, S., Liang, M., Naqvi, N. I., Lin, C., Qian, W., Zhang, L. H., & Deng, Y. Z. (2017). Phototrophy and starvation-based induction of autophagy upon removal of Gcn5-catalyzed acetylation of Atg7 in *Magnaporthe oryzae*. *Autophagy*, *13*(8), 1318–1330.

Zhao, C., Li, Y., Qiu, W., He, F., Zhang, W., Zhao, D., … hu, Y. (2018). C5a induces A549 cell proliferation of non-small cell lung cancer via GDF15 gene activation mediated by GCN5-dependent KLF5 acetylation. *Oncogene*, *37*(35), 4821–4837.

How to cite this article: Jiang R, Zhang Z, Zhong Z, Dai Y, Liu G, Zhang C. Phosphorylation of histone H4 at serine 1 is associated with GCN5 and mediates autophagy in osteosarcoma bone cell lines. *J Cell Physiol*. 2020;1–9. https://doi.org/10.1002/jcp.29434